Stress fields and energy of disclination-type defects in zones of localized elastic distortions

Ivan I. Sukhanov, Alexander N. Tyumentsev, and Ivan A. Ditenberg

Citation: AIP Conference Proceedings **1783**, 020220 (2016); doi: 10.1063/1.4966514

View online: http://dx.doi.org/10.1063/1.4966514

View Table of Contents: http://scitation.aip.org/content/aip/proceeding/aipcp/1783?ver=pdfcov

Published by the AIP Publishing

Stress Fields and Energy of Disclination-Type Defects in Zones of Localized Elastic Distortions

Ivan I. Sukhanov[1,2,a)], Alexander N. Tyumentsev[1,2,3], and Ivan A. Ditenberg[1,2,3]

[1] *National Research Tomsk State University, Tomsk, 634050 Russia*
[2] *Siberian Physical-Technical Institute, Tomsk, 634050 Russia*
[3] *Institute of Strength Physics and Materials Science SB RAS, Tomsk, 634055 Russia*

[a)] Corresponding author: suhanii@mail.ru

Abstract. This paper studies theoretically the elastically deformed state and analyzes deformation mechanisms in nanocrystals in the zones of localized elastic distortions and related disclination-type defects, such as dipole, quadrupole and multipole of partial disclinations. Significant differences in the energies of quadrupole and multipole configurations in comparison with nanodipole are revealed. The mechanism of deformation localization in the field of elastic distortions is proposed, which is a quasi-periodic sequence of formation and relaxation of various disclination ensembles with a periodic change in the energy of the defect.

INTRODUCTION

Representations of the rotational modes of deformation, partial disclinations, their dipoles and multipoles as the carriers of plastic deformation and lattice reorientation in metal alloys have been developed since the middle of the 1970s [1]. Micromechanisms of these deformation modes are analyzed using cooperative dislocation models of the formation and evolution of disclination-type defects [2]. In works [3, 4] the possibility of the formation of nanodipoles of partial disclinations in the field of elastic distortions is shown. The formation of these defects is not associated with collective dislocation phenomena. In this paper, a theoretical study of the elastically deformed state and energies of these disclination-type defects in the above mentioned zones is conducted.

MATERIALS AND EXPERIMENTAL PROCEDURES

The computing experiment and visualization of stress fields and spatial distribution of elastic energy were conducted in computer algebra system Maple version 15. The simulation of tension fields was carried out using an explicit form of the stress tensor components [5]. The dependence of the energy of disclination configurations (dipole/quadrupole) was analyzed using numerical integration by the Gauss method in the adaptive 30-point variation. The integration values were estimated using the Kronrod rule for 61 ponts.

The crystal was simulated based on the representations of a homogeneous isotropic continuum for which the Hooke's law is valid. The independent elastic constants were the shear modulus (G) and Poisson's ratio (ν). The value of the Frank's vector (power of disclinations) ω during computing experiments did not change and amounted to $\omega \approx 1°$.

RESULTS AND DISCUSSION

A detailed electron microscopic analysis represented in Fig. 1 was conducted elsewhere [3]. The scheme of misorientations that form the diffraction contrast of the crystal lattice planes in section *AB* is shown in Fig. 1b. As can be seen from this scheme, when the specific values of widths of nanobands and the angles of reorientation in them are $\Delta r \approx 3$–5 nm and $\Delta\varphi \approx 1°$ respectively, then the gradient of crystal orientation in the zone of nanoband ($\Delta\varphi/\Delta r$) is several hundreds of degrees per micrometer.

Advanced Materials with Hierarchical Structure for New Technologies and Reliable Structures 2016
AIP Conf. Proc. 1783, 020220-1–020220-5; doi: 10.1063/1.4966514
Published by AIP Publishing. 978-0-7354-1445-7/$30.00

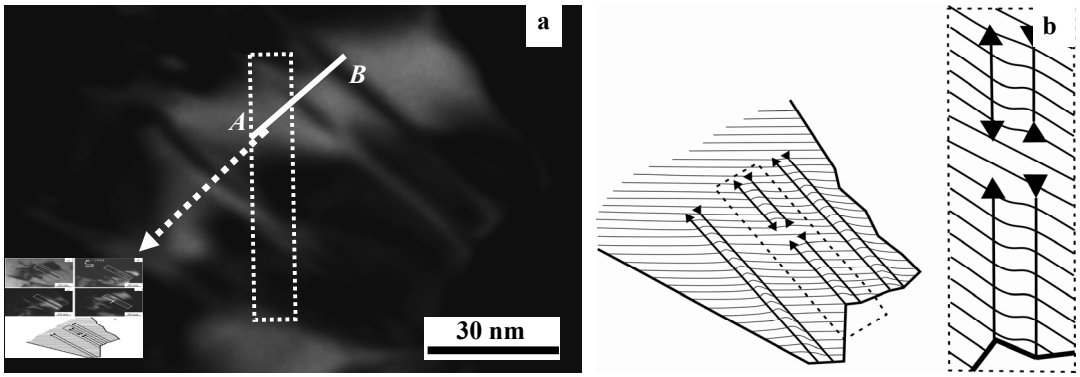

FIGURE 1. Reorientation nanobands in nickel after deformation by torsion under pressure $e \approx 5$ [5]. Electron microscopic image in the dark field (a); scheme of nanodipoles of partial disclinations (b)

The enlarged image of the analyzed area presented in the lower left corner of Fig. 1a illustrates the smooth nature of change in the extinction contour intensity, indicating the absence of localized boundary misorientation in this region. Therefore, we deal with a continuous change of crystal orientation at the crystal lattice curvature $\chi_{ij} \approx 200°–300°$ μm^{-1} (Fig. 1b). The absence of any features of dislocation contrast in the zones of nanobands is an evidence of the elastic nature of this curvature.

Thus, an important feature of the mechanical behavior of nickel in submicrocrystalline state during torsion on Bridgman anvils is the localization of deformation in the field of elastic distortions. This feature is obviously the ability of nanoobjects of size of a few nanometers (in our case, reorientation nanobands) to generate structural states with high (hundreds of degrees per micrometer) elastic curvature of the crystal lattice at relatively low values of local internal stresses. These stresses can be estimated using the formula $\sigma_{loc} \approx \chi_{ij} E \Delta h/2$, where E is the Young's modulus and Δh is the characteristic sizes of the zone of curvature. According to this formula, in nanoobjects of size of a few nanometers (at $\Delta h \approx 3–5$ nm) these stresses ($\sigma_{loc} \approx E/220–E/360$) are considerably below the yield point of the material in the nanostructured state.

The latter is valid in local zones within nanobands. At the front of their distribution in the nanodipole zone the magnitude of local internal stresses is much higher. The results of their theoretical assessment for the nanodipole of wedge disclinations with the experimentally determined values in Fig. 1 $l \approx 6$ nm and $\varphi \approx 1°$ are shown in Fig. 2. As is seen, the maximum values $P \approx \pm E/50$ (E is the Young's modulus) are observed in the bedding plane of the nanodipole (in the section $y = 0$). With the increasing distance from this plane up to 1 and 3 nm the values of pressure are reduced to $P \approx E/100$ and $E/300$, respectively.

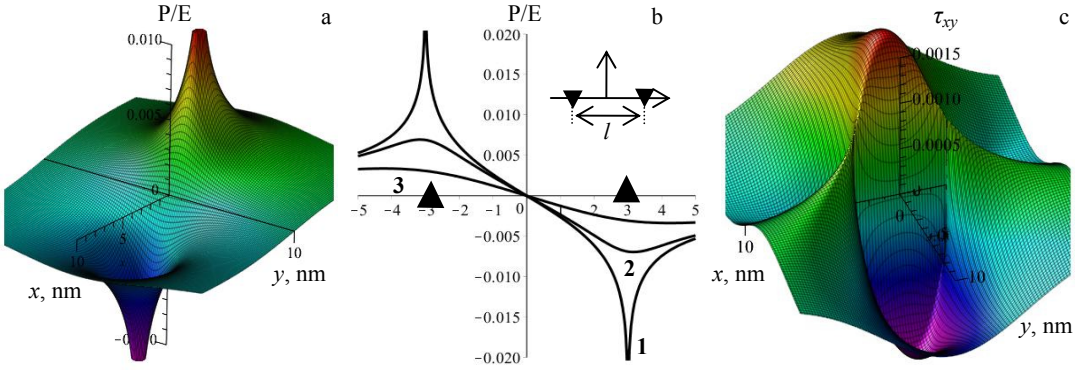

FIGURE 2. Spatial distribution of pressure $P = (\sigma_{11} + \sigma_{22} + \sigma_{33})/3$ for the nanodipole of partial wedge disclinations with the shoulder size $l = 6$ nm and Frank's vector $\omega \approx 1°$ (a), its projections at different distances from the bedding plane of the dipole $y = 0$ nm (*1*), $y = 1$ nm (*2*), $y = 3$ nm (*3*) (b), and component τ_{xy} of the nanodipole stress tensor with the parameters $l = 6$ nm, $\omega \approx 1°$ (c)

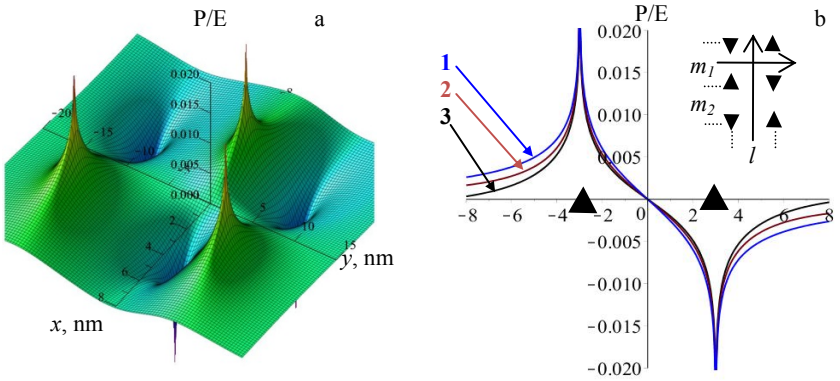

FIGURE 3. Spatial distribution of pressure $P = (\sigma_{11} + \sigma_{22} + \sigma_{33})/3$ for the nanodipole of partial wedge disclinations with parameters $l = m_1 = 6$ nm, $m_2 = 12$ nm, $\omega \approx 1°$ (a) and its projections on the plane $x0P$ of maximum stresses in the sections: $y = 0$ nm (*1*), $y = 6$ nm (*2*), $y = -12$ nm (*3*) (b)

Thus, the nature of the elastically deformed state in the neighborhood of a nanodipole is qualitatively different from that in the nanoband formed in the process of its propagation. In the nanoband already at the distance 3 nm from the nanodipole internal stresses are much lower than the yield point. In the nanodipole plane they are nearly an order of magnitude higher. At small sizes of the nanodipole shoulder these stresses provide very large pressure gradients ($\partial P/\partial x \sim (10–20)E$ μm^{-1}) in its plane.

Another important feature of the nanodipole stress field is that the maximum value of the stress tensor components τ_{xy} is located ahead of the front of the moving dipole. In our opinion, this fact is a significant energy factor in the formation of quadrupole configurations at the front of propagating reorientation nanobands (Fig. 2c). This leads to more complicated multipole configurations that represent a system of interacting quadrupoles.

Based on the experimental data, for the analysis of stress fields as the studied system we chose a multipole with the distance between quadrupole and dipole $m_1 = 6$ nm and quadrupole length $m_2 = 12$ nm (Fig. 3a). As is seen from Fig. 3, the multipole configuration is a complex shielded system with preferred localization of stress fields in the field of the bedding of disclinations with the maximum values $P \approx E/50$.

Since the analyzed disclination configurations are “defects” of an elastically strained medium, an important issue is their stability. Firstly, the stability is determined by the stresses that exist in the vicinity of the defect and preserve this defect. In particular, these can be the local stresses of the nanocrystal boundary emitting this defect. Secondly, it depends on the value of the strain energy reserved by the defect. In this regard, a comparative analysis of specific elastic energy distribution in the continuum for disclination configurations formed during propagation of nanodipole of partial disclinations has been conducted. The results of this analysis are represented in Fig. 4.

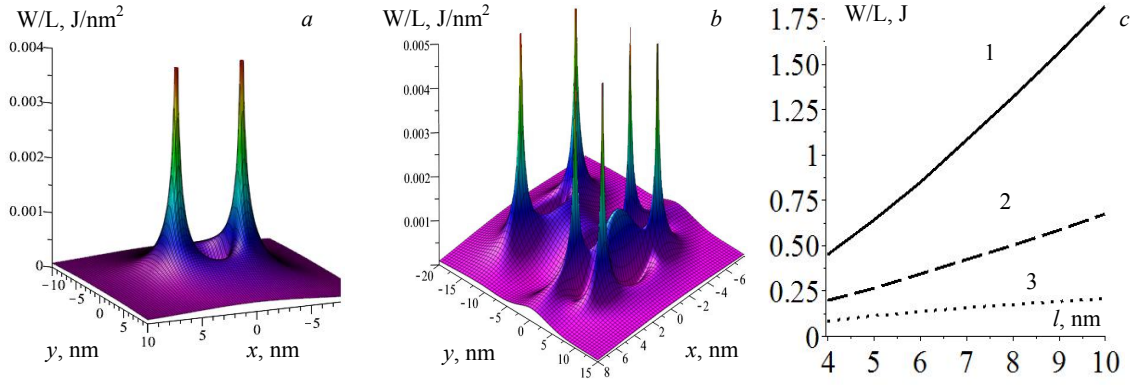

FIGURE 4. Spatial distribution of specific elastic energy for the nanodipole of partial wedge disclinations with parameters $l = 6$ nm, $\omega \approx 1°$ (a) and the multipole of partial disclinations with parameters $l = m_1 = 6$ nm, $m_2 = 12$ nm, $\omega \approx 1°$ (b); energies of nanodipole (*1*), quadrupole with fixed shoulder $m = 6$ nm (*2*) and multipole with fixed shoulders $m_1 = 6$ nm, $m_2 = 12$ nm (*3*) (c)

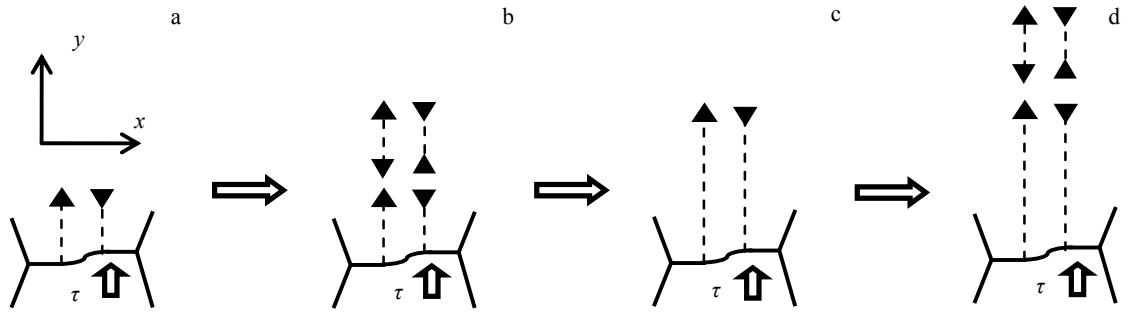

FIGURE 5. Schematic motion of nanodipole of partial disclinations

The calculation of energies of disclination configurations has shown that there are significant differences in the energies of quadrupole as well as multipole configurations compared to nanodipole in a wide range of quadrupole sizes (lengths). At the same time, the energy of the multipole configuration has several times lower energy as compared to the nanodipole.

The following results are important for the analysis of the mechanism of deformation localization in the field of elastic distortions.

1) The origin of nanodipoles of partial disclinations in the zones of localized elastic distortions occurs at the nanograin boundaries.

2) A significant energy reduction in the system of nanodipoles of partial disclinations due to a decrease in the nanodipole shoulder size or width of a nanoband of localized elastic distortion at a constant value of the total shear.

3) Despite the high value of P and corresponding components σ_{ii}, the leading role in the formation of localized deformation nanobands in the field of elastic distortions plays the shear component of the stress tensor τ_{xy} (Fig. 5).

4) Quadrupoles of partial disclinations are formed ahead of the front of the propagating nanodipole under the effect of this component, leading to multipole configurations with a multiple decrease in the defect energy.

In view of the above mentioned results, the formation mechanism of nanobands of localized elastic distortion, including the following stages (Fig. 5), is possible.

Stage I: The generation of a nanodipole of partial disclinations on the nanocrystal boundary under the influence of the shear component of the stress tensor τ_{xy} (Fig. 5a). The feature of this stage is that at a constant value of the total shear the smaller is the shoulder size of the nanodipoles entering into the formed disclination ensemble, the lower is the energy of this ensemble. The formation of an opposite-sign nanodipole on the grain boundary, which leads to the formation of quadrupoles with much lower energy of the disclination ensemble can be an energy factor of decrease in this energy.

Stage II: The formation of a quadrupole of partial disclinations in the zone ahead of the front of a propagating nanoband (Fig. 5b). This stage is a consequence of the specific nature of the stress field of nanodipole, namely, the presence of the maximum shear component of stresses in this zone. An important feature of this stage is that it is accompanied by a considerable (more than twice) reduction of defect energy.

Stage III: The combination of the quadrupole with the moving nanodipole (Fig. 5c).

Further motion of the nanodipole is carried out by multiple reiterations of stages II and III.

In the conditions of the above described mechanism the nanodipole of partial disclinations represents a unique stress concentrator, determining its motion in the direction of the maximum values τ_{xy}. In our opinion, this feature is an important factor providing the possibility of deformation localization with the formation of nanobands of elastic shear and rotations discussed here. An extremely important fact is that its motion on stage II is accompanied by a multiple decrease of defect energy.

In conclusion we note that within the given above mechanism the defect as a carrier of deformation in the considered field of localized elastic distortions is not simply a nanodipole of partial disclinations. It is a more complex ensemble of disclinations whose structure (quadrupoles and multipoles of partial disclinations) periodically changes during deformation, as well as with the periodic decrease in energy. We thus deal with a quasi-wave nature of propagation of elastic distortions (shear and rotations) in a crystal during nanoband formation.

SUMMARY

A characteristic feature of the zones of localized elastic distortions is the highest values of the diagonal components of the stress tensor and their gradients and localization of the maximum value of shear components of this tensor ahead of the front of nanodipole propagation. An impetus for deformation localization in the field of elastic distortions is a significant decrease in the energy of the disclination ensemble with the reducing size of nanodipoles forming it. The mechanism of deformation localization in the field of elastic distortions was proposed which is a quasi-periodic sequence of formation and relaxation of various disclination ensembles with a periodic change in defect energy.

ACKNOWLEDGMENTS

The work was conducted within the framework of the Basic Research Program of the State Academies of Sciences for 2013–2020 at partial financial support of Tomsk State University Competitiveness Improvement Program. Investigation was carried out using the equipment of the Tomsk State University.

REFERENCES

1. A. N. Vergasov, V. A. Likhachev, and V. V. Rybin, Phys. Met. Metallogr. **42**, 146–154 (1976).
2. V. I. Vladimirov and A. E. Romanov, *The Physical Nature of Metals Fracture* (Metallurgy, Moscow, 1984).
3. A. N. Tyumentsev and I. A. Ditenberg, Phys. Mesomech. **14**(5–6), 249–260 (2011).
4. A. N. Tyumentsev and I. A. Ditenberg, Russ. Phys. J. **54**, 26 (2011).
5. V. I. Vladimirov and A. E. Romanov, *The Disclinations in Crystals* (Nauka, Leningrad, 1986).